Discharge Characteristics of Piano Key Weirs With and Without Upstream Siltation

Abstract: The application of a piano key (PK) weir in a channel may lead to changes in the flow characteristics, upstream siltation conditions, and bed elevation. In this study, laboratory-based Type-A PK weir models with noses below the upstream apexes were studied under different flow and siltation conditions. A total of 342 datasets were collected from the three models. Upstream siltation had no impact on the discharge efficiency of submerged PK weirs, but under the free-flow condition, there was a maximum reduction of 4% in the coefficient of discharge. Planners and designers must consider such variations in channels with a high sediment load. However, at high H/P (where H is the head over the weir crest and P is the weir height), the siltation effect starts to decrease, possibly due to the alternation in the flow condition caused by tailwater submergence. The modular submergence was found to be approximately 0.5, which is close to the values available in the literature. The proposed equations for free-flowing PK weirs performed very well with a maximum error of approximately 7% and a mean absolute percentage error (MAPE) of approximately 2.5%. Furthermore, approximately 60% of the data lie within the ± 3% error bands, and almost all data lie within the ± 6% error bands. The equations proposed for submerged PK weirs also efficiently estimated the coefficient of discharge with a maximum error ranging from 9.0% to 11.32% and an MAPE varying from 2.94% to 4.27%.

Keywords: Discharge capacity, Experimental study, Piano key weir, Siltation.

1 Introduction

A piano key (PK) weir is a relatively new type of non-rectilinear spillway that is often preferred over conventional weirs such as sharp-crested weirs, ogee-crested weirs and labyrinth weirs to augment the discharge capacity of low-head dams and diversion structures. This type of modified labyrinth weir is superior to other weirs due to its ability to pass flood water at a much higher specific discharge and its smaller constructional footprint [1,2]. With an increase in the design flood level due to climate change, it has become essential to enhance the discharge capacities of old ogee-crested and traditional labyrinth weirs. Over the past decade, PK weirs were generally constructed over the crest at dams with low heads to enhance the overflow capacity of the existing dams [3]. A PK weir has a longer effective crest length, which helps it to increase the discharge capacity [2,3]. In addition, a PK weir is free-flowing; that is, there is no need to operate a mechanical gate. Thus, PK weirs are more economical than gated weirs and avoid catastrophic dam failures caused by the malfunctioning of gates or faulty operation. In a few areas, such as Van Phong (Vietnam), Sawra-Kuddu (India), and Giritale (Sri Lanka), PK weirs have been constructed as diversion or control structures [4,5]. However, upstream (u/s) sedimentation and changes in channel morphology may arise when such structures are implemented. During a high flood event, a PK weir could transport a major amount of incoming sediment [5].

The concept of the PK weir was primarily envisaged by Hydrocoop (a non-profit organisation) in association with Biskra University (Algeria), the Hydraulic Laboratory of Electricité de France (EDF, France) and the Indian Institute of Technology Roorkee (India) at the beginning of the 21st century to enhance the performance of existing weirs [6,7]. Lempérière and Ouamane [2] found that a PK weir can enhance the discharge capacity of existing traditional spillways by several times at the same head. The PK weir constructed at the Goulours dam, France, in 2006 was the first prototype [6]. To date, many PK weirs have been built across the globe, mostly in France and Vietnam [7]. A recent study showed that approximately 34 PK weirs and 100 labyrinth weirs have been constructed [8]. There are four types (A, B, C and D) of PK weirs depending on the upstream and downstream (d/s) overhangs [7,9,10]. The plan and longitudinal sections of a three-cycle (Type-A) PK weir with noses below the upstream apexes are shown in Fig. 1, where a and b are the inlet and outlet key widths, respectively; B is the sidewall overflowing crest length; B_i and B_o are the inlet and outlet overhang lengths, respectively; B_b is the base length along the flow; P is the weir height = inlet key height P_i = outlet key height P_o; P′ is the incoming flow depth below the key sill; T_s is the thickness of the sidewalls; and W is the channel width. The discharge equation of a PK weir [10] can be expressed as

$$Q = \frac{2}{3} C_{PK} W \sqrt{2gH^3} \quad (1)$$

where Q is the discharge; C_{PK} is the coefficient of discharge for the PK weir; g is the acceleration due to gravity; and H is the head over the weir crest (including the velocity head h_v).

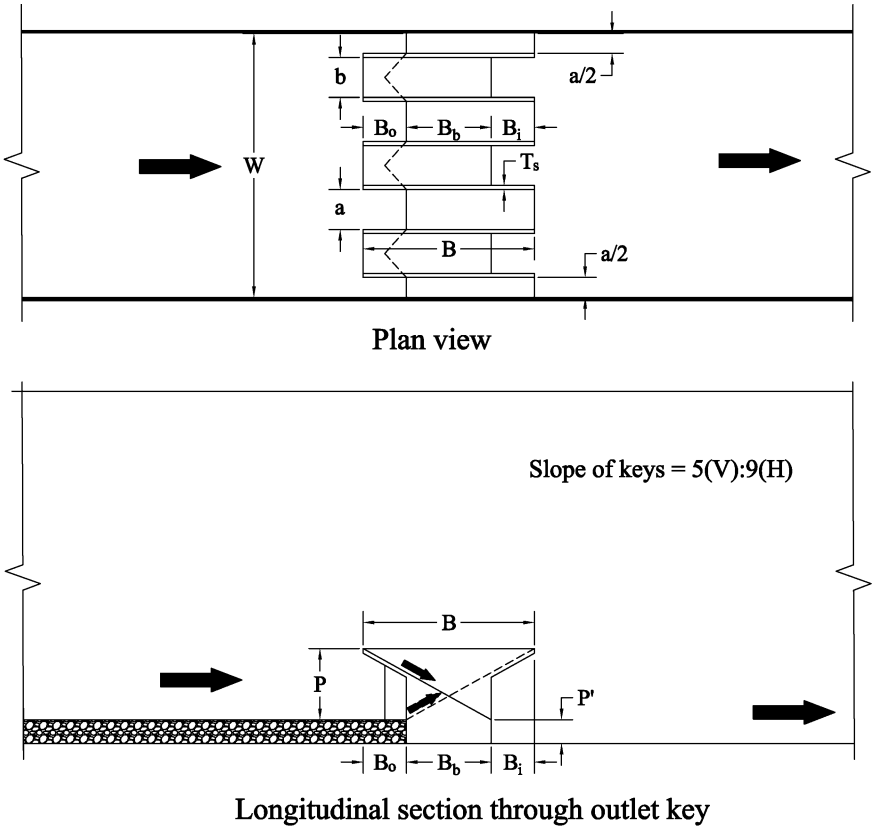

Fig. 1 Plan and longitudinal views of a PK weir with noses

For two decades, research on PK weirs has focused mostly on their discharge capacity and the effects of different geometric parameters on the discharge capacity [7,11]. A few notable studies on this topic were carried out by Anderson and Tullis [12,13], Belaabed and Ouamane [14], Cicero and Delisle [15], Crookston et al. [16], Kabiri-Samani and Javaheri [10], Karimi Chahartaghi et al. [17], Kumar et al. [18], Laugier et al. [19], Leite Ribeiro et al. [1,3], Lempérière [20], Li et al. [21], and Machiels et al. [22–24]. However, scarce literature is available that focuses on the effect of upstream siltation on the discharge capacity of PK weirs placed in-channel. Researchers have observed that L/W (directly proportional to C_{PK}), where L is the total crest length of the PK weir, and H/P (inversely proportional to C_{PK}) are the most important parameters affecting C_{PK}, followed by other parameters such as a/b, B/P, P/a, P/W_u (where W_u is the width of a PK weir unit = a+b+2T_s), B_i/B, and B_o/B [1,3,7,10,24]. Along with these primary parameters, other important factors are the parapet wall, the presence of noses beneath the upstream apexes, the shape of the crest, submergence, and floating debris.

Lempérière [20] proposed a simplified empirical equation for the unit discharge that depends on the weir height and water head based on a model study with L/W = 5, a/b = 1.25, B_i/B = 0.5 and $0.27 \leq H/P \leq 1.3$. Machiels et al. [22] proposed a preliminary design method for PK weirs by extrapolating available experimental datasets. Leite Ribeiro et al. [1] performed laboratory experiments on scaled physical models and suggested an empirical formula for the discharge increase ratio of a Type-A PK weir compared to a linear sharp-crested weir considering primary and secondary parameters. Based on the data collected from previous experiments, Leite Ribeiro et al. [3] suggested a systematic design approach for PK weirs and indicated the importance of L/W, H/P, P/a and P/P′ in modulating the design discharge; however, the effect of P/P′ could not be analysed using the available data. Anderson and Tullis [13] conducted a series of experiments and compared the hydraulic performance between a PK weir and a rectangular labyrinth weir with sloping key floors; a maximum increased efficiency of 9.3% and a mean increase of 8.2% were found for the PK weir, and this enhancement was attributed to the overhanging keys of the PK weir that reduce the inlet velocity and head loss due to the larger wetted perimeter. Similarly, Type-B PK weirs have a higher discharge efficiency than other types [10]. PK weirs with noses below the outlet apexes pass higher amounts of discharge than regular PK weirs [12,14]. Anderson and Tullis [12] studied the effects of a/b, the presence of noses beneath the upstream apexes, the parapet wall and the crest shape using a large number of flume models and suggested that the optimum value of a/b ranges from 1.25 to 1.5. A higher discharge efficiency was observed with an increase in a/b and in the presence of noses, a parapet wall and a rounded crest. Noses beneath the upstream apexes provide a smooth flow transition and reduce the inlet energy loss, and thus, an enhancement (maximum of 2.8% for the model

with a/b = 1.25) in the discharge capacity was found. In contrast, Anderson and Tullis [12] observed a 13.3% increase in the discharge capacity by installing a parapet wall, which not only reduces the inlet loss but also decreases the outlet submergence. However, a parapet wall increases the weir height and discharge capacity only when the weir height is less than the optimum design value [23]. Therefore, Machiels et al. [23] suggested using a parapet wall in a rehabilitation project to augment the discharge capacity of an existing PK weir by up to 20% with a marginal rise in the maximum water level. Cicero and Delisle [15] conducted experiments for both free-flow and submerged flow conditions on Type-A, Type-B and Type-C PK weirs to study the influences of hangovers (upstream and downstream) on the efficiency and coefficient of discharge of PK weirs. It was found that Type-B weirs are more efficient (5-10% under the free-flow condition) than Type-A weirs, but Type-C weirs are less efficient (approximately 15% under the free-flow condition) than Type-A weirs. Kabiri-Samini and Javaheri [10] conducted experiments on thirty PK weir models with a wide range of parameters and derived empirical formulae for the coefficient of discharge of different PK weir types under both free-flow and submerged flow conditions. Pfister et al. [25] carried out experimental investigations to establish the association among several PK weir configurations and different-sized timbered wreckages of varying shape; a 50% jamming probability was observed if the driftwood diameter was equal to the PK weir's critical flow depth. Machiels et al. [24] suggested separate design guidelines for new and rehabilitation projects. For a new PK weir with L/W = 5, the maximum discharge capacity could be attained when $P/W_u = 1.3$, a/b = 1.25 and $B_o/B_i = 3$ (higher upstream overhang), whereas due to limitations in the height of demolition work, $P/W_u \approx 0.5$ was suggested for rehabilitation work while keeping a/b and B_o/B_i equal to 1. Using their own and other experimental datasets ($4.6 \leq L/W \leq 6$, $0.1 \leq H/P \leq 0.9$), Kumar et al. [18] found that the equations of the coefficient of discharge proposed by Crookston et al. [16] and Cicero and Delisle [15] are more accurate than the equations presented by other researchers. Karimi Chahartaghi et al. [17] carried out an experimental study on sixteen arced PK weir models and observed a maximum enhancement of 10% in the discharge capacity because of a parapet wall. Li et al. [21] observed that a PK weir with a/b > 1.0 has a much higher discharge capacity than a model with a/b < 1.0, but the difference decreases with a rise in the head. Noseda et al. [5] conducted a study on scouring upstream of a PK weir and investigated its self-cleaning capability. It was found that partial filling of the inlet keys leads to a substantial reduction in the discharge capacity.

The submergence of a weir may be defined as the condition at which the tailwater level rises above the crest level. Submergence (S_w) can be represented as the ratio of the total downstream head above the crest H_d to the total upstream head above the crest H, i.e., $S_w = H_d/H$ [10,26,27]. Generally, an increase in weir submergence leads to a decrease in the coefficient of discharge [10,14,15,26–29]. Dabling and Tullis [26] carried out a study on the submergence of a PK weir and compared it with that of a labyrinth weir and observed that the PK weir has a higher discharge efficiency than the labyrinth weir at low submergence, i.e., $S_w < 0.55$. Kabiri-Samani and Javaheri [10] suggested an empirical formula for submerged PK weirs considering the parameters S_w (> 0.6) and L/W ($2.5 \leq L/W \leq 6$). A negligible effect of submergence on C_{PK} was observed by Dabling and Tullis [26] for $S_w < 0.48$ and by Kabiri-Samani and Javaheri [10] for $S_w < 0.6$; this range is called modular submergence. In the case of Cicero and Delisle [15], the modular submergence limits were 0.2, 0.5 and 0.6 for Type-B, Type-A and Type-C weirs, respectively. A Type-B PK weir was deemed more efficient than a Type-A weir only up to $S_w < 0.5$. Therefore, an increase in the upstream overhang enhances the submergence effect. A similar outcome was reported by Belaabed and Ouamane [14].

It is evident from the aforementioned literature that earlier investigations were carried out without considering the case of siltation upstream of the PK weir. Furthermore, under sediment-laden channel-type flow, sediment may be deposited up to the sill of the inlet key of a PK weir, i.e., P′ as shown in Fig. 1. Triangular noses up to half of the outlet overhangs were fabricated and fitted onto the models investigated herein for a smooth flow transition. The present investigation is conducted to investigate the effect of upstream siltation up to the sill height on the discharge capacity of a PK weir with noses below the upstream apexes under different flow conditions. Moreover, empirical equations are suggested to estimate the discharge capacity of PK weirs with and without upstream siltation under free-flow and submerged flow conditions. The upstream siltation considered in the study extends up to the sill level of the keys.

2 Dimensional analyses

The discharge capacity of a free-flowing weir depends mainly on several geometric, flow and fluid parameters. The coefficient of discharge for a free-flowing PK weir can be expressed as

$$C_{PK} = f(H, L, P, P', W, a, b, V, g, \rho, \sigma, \mu) \quad (2)$$

where f is the functional symbol, L is the total crest length of the weir, and V is the flow velocity. On applying dimensional analysis and rearranging the terms, one can obtain

$$C_{PK} = \varphi\left(\frac{L}{W}, \frac{a}{b}, \frac{H}{P+P'}, \frac{V}{\sqrt{gy}}, \frac{\rho V^2 y}{\sigma}, \frac{\rho V y}{\mu}\right) \quad (3)$$

where φ is another functional symbol and the flow depth y = H+P+P′. Surface tension and viscosity are two properties of fluids that cannot be scaled, and thus, scale effects occur at low head over the crest; therefore, sufficiently high Reynolds numbers and Weber numbers are required to eliminate these scale effects [1,3,30,31]. The minimum value of H to eliminate the scale effects for a PK weir was found to be within 0.03 m by Erpicum et al. [30], Tullis et al. [31] and many other researchers, as mentioned in Tullis et al. [31]. Only datasets having a head ≥ 0.03 m over the weir crest are used in the present study. Therefore, the scale effects are negligible, the surface tension effect on C_{PK} is small, and the Weber number is eliminated from the analysis as per Novak and Cabelka [32] and Kabiri-Samani-Javaheri [10]. Additionally, the Reynolds number is eliminated because the effect of viscosity is small in comparison with the effect of gravity in the case of turbulent flow [10,33]. Further, this type of flume model study is conducted under subcritical flow conditions while following a Froude similitude, where the effects of gravity are well represented [3]. Thus, the Froude number was eliminated from the analysis. Additionally, the effect of the incoming flow velocity has already been included in H (as the velocity head h_v). In the present study, the variation in a/b (from 1.124 to 1.226) is small, and therefore, its effect is small and thus omitted from the analysis. With these considerations, Eq. (3) can be rewritten as

$$C_{PK} = \varphi\left(\frac{L}{W}, \frac{H}{P+P'}\right) \quad (4)$$

Under submerged flow conditions, the downstream head above the crest H_d or (eventually) the submergence mostly affects the discharge capacity of PK weirs. A considerable effect of L/W was also observed in a previous study [10]. A functional relationship for the coefficient of discharge under submergence C_{PKs} may be written as

$$\frac{C_{PKs}}{C_{PK}} = \psi\left(\frac{H_d}{H}, \frac{L}{W}\right) \quad (5)$$

where ψ is the functional symbol. The free-flow and submerged flow conditions for a PK weir with noses below the outlet overhangs are shown in Figs. 2a and 2b. Villemonte [29] adopted the principle of superposition and used experimental results to establish a simplified correlation for the flow reduction factor of submerged sharp-crested weirs as [27]

$$\frac{Q_s}{Q} = c_1\left(1 - \left(\frac{H_d}{H}\right)^{a_1}\right)^{b_1} \quad (6)$$

where Q_s is the flow passing over a submerged weir and a_1, b_1 and c_1 are coefficients. Villemonte [29] found c_1 = 1.0 for seven tested weir types for a range of submergence values between 0 and 0.9. This relationship may also be used for PK weirs to establish a simplified correlation between the flow passing over submerged PK weirs and the submergence.

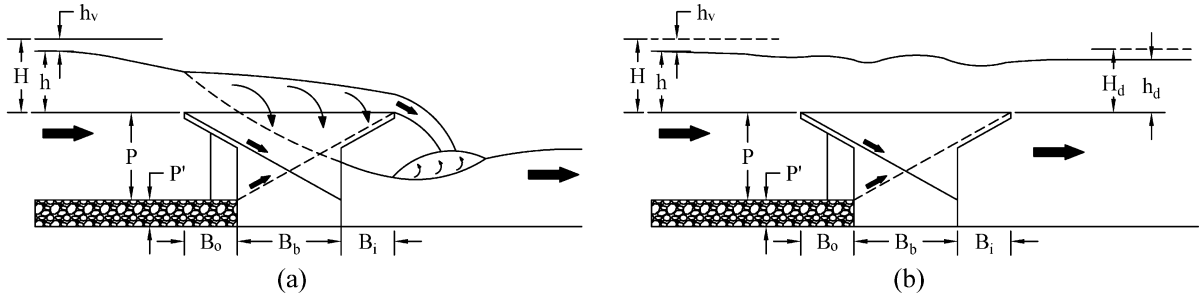

Fig. 2 a Free-flowing PK weir with noses, and **b** Submerged flowing PK weir with noses [10,18]

3 Experiments

Experiments were carried out to study the discharge capacity of PK weirs under free-flow and submerged flow conditions. The effect of siltation upstream of the PK weirs on their discharge capacity was also investigated. Tests were performed for different dimensions of the PK weir, values of discharge and upstream siltation conditions. All the experiments were performed in the Hydraulics Laboratory of the Department Civil Engineering, IIT Roorkee, in a 15.0 m long, 0.39 m wide and 0.5 m deep tilted flume. A major section of the flume was equipped with glass walls to ensure proper visualisation of the flow. A schematic plan of the flume is shown in Fig. 3a. Honeycomb grid walls, flow straighteners and a wave suppressor are provided upstream of the flume to minimise flow disturbance and cross-currents. An ultrasonic flowmeter (accuracy ± 1%) and point gauge (least count = 0.0001 m) were used to record discharge and head, respectively. Such precise measurement techniques have minimised the uncertainty in measurement. The flowmeter was connected to the inlet pipe. The discharge varied from 8.3×10^{-3} m^3/s to 33.4×10^{-3} m^3/s in the study.

Three PK weir models with different numbers of cycles/units and having noses below the outlet apexes were fabricated from a 0.006 m thick acrylic sheet, as shown in Fig. 3b. The dimensions of the models are listed in Table 1. The experimental model dimensions are comparable to the models used in the previous studies carried out by Jüstrich et al. [34], Leite Ribeiro et al. [3], Noseda et al. [5], and Tullis et al. [31]. To study the effect of siltation on the discharge capacity, one set of sediment (gravel mixture) with a median size (d_{50}) of 0.0055 m was placed upstream of the PK weir up to the sill of the inlet key (P´= 0.035 m). The gravels were mostly rounded, and the specific gravity was 2.64. The gravel size used in the present study is comparable to the gravel size used by Jüstrich et al. [34] (d_{50} = 0.0063 m) and Noseda et al. [5] (d_{50} = 0.0069 m) in their studies related to scouring around PK weirs. Further, the parameter d_{50}/P = 0.052 in the present study was within the range of $0.01 \leq d_{50}/P \leq 0.08$, as indicated in Noseda et al. [5]. The tailgate was used to vary the downstream water level. A total of 342 datasets were collected in the present experimental study. The water level on the upstream side was measured 0.2 m upstream of the outlet key, whereas on the downstream side, the elevation was measured under the submerged flow condition 1.1 m downstream of the inlet key. In the present study, a total of four equations, Eqs. (7), (8), (9) and (10) are established depending on the flow condition, upstream siltation and other parameters, as listed in Table 2.

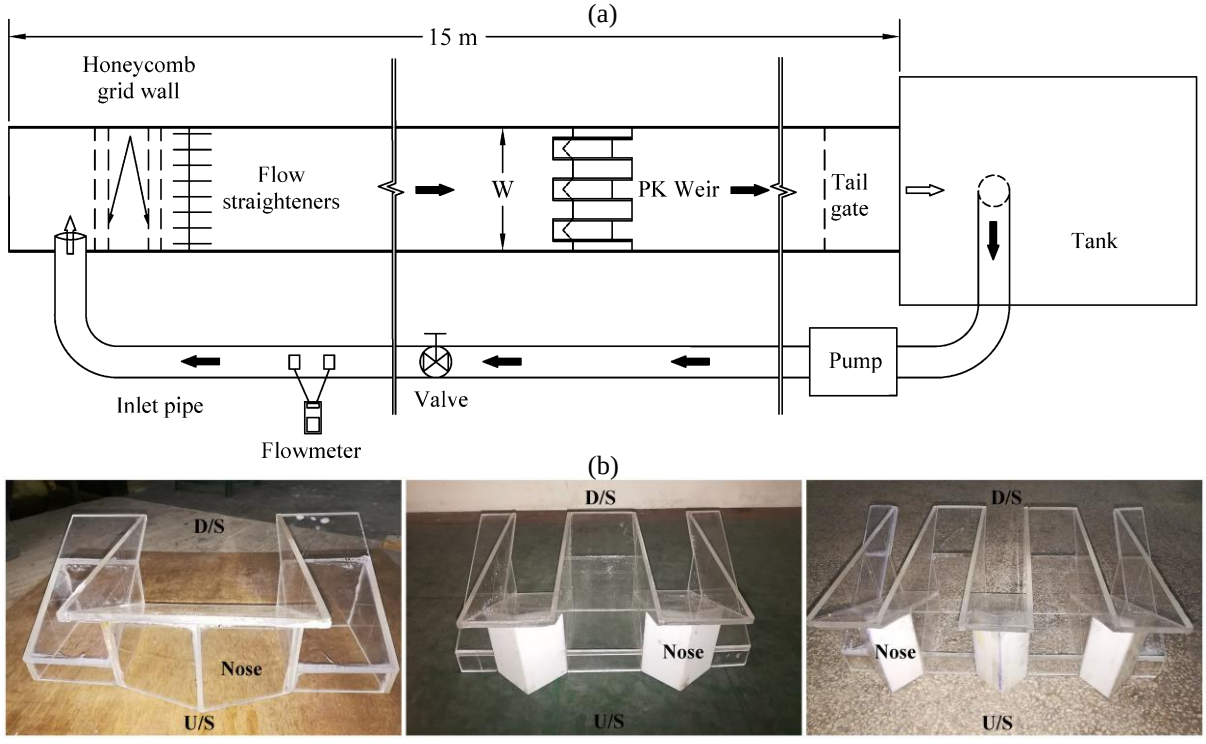

Fig. 3 a Schematic plan of the experimental setup, and **b** Three PK weir models with noses

Table 1
Detailed dimensions of the PK weirs

Model	No. of cycles	L(m)	W(m)	P(m)	a(m)	b(m)	B_b(m)	$B_i = B_o$(m)	$S_i = S_o$
PKN_1	One	0.898			0.2	0.178			
PKN_2	Two	1.402	0.39	0.105	0.1	0.083	0.125	0.064	5(V):9(H)
PKN_3	Three	1.908			0.065	0.053			

Table 2
Applicability of different equations

Equation no.	Siltation	Flow	#Total datasets	L/W	H/P	H/(P+ P′)	H_d/H
7	No	Free	69	2.3 – 4.9	0.29 – 0.89	0.21 – 0.65	–
8	No	Submerged	104		–	–	0.117 – ≈1.0
9	No	Submerged	66		–	–	0.117 – 0.9
10	Up to the sill of the key	Free	67		0.29 – 0.9	–	–

Note#: The total number of datasets collected in the study = 69 + 104 + 67 + 102 (with upstream siltation under submerged flow) = 342.

4 Results and discussion

4.1 Proposed equations for the coefficient of discharge under the free-flow condition

A total of 46 datasets collected in the current experimental study were used to establish the relationship for the coefficient of discharge under the free-flowing condition. Using the least squares technique, the following equation was developed:

$$C_{PK} = 0.619 \left(\frac{L}{W}\right)^{0.378} \left(\frac{H}{P+P'}\right)^{-0.354} \qquad (R^2 = 0.973) \qquad (7)$$

The coefficient of determination (R^2) for Eq. (7) is 0.973. The remaining 23 datasets were used to validate Eq. (7). Figure 4 shows a comparison of the computed C_{PK} using Eq. (7) with the observed values both for training and for validation. It was found that approximately 60.9% and 65.2% of the training and validation data, respectively, lie in the ± 3% error bands, while 97.8% and 95.7% of the data lie in the ± 6% error bands. The maximum error and mean absolute percentage error (MAPE) for the 23 datasets used in the validation are 7.0% and 2.5%, respectively, and the root mean square error (RMSE) is 0.045. Therefore, Eq. (7) performs very well.

The parameters used to derive Eq. (7) were analysed to determine the sensitivity of the proposed equation to these parameters. The R^2 values for different combinations of independent variables are given in Table 3, which indicates that both L/W and H/(P+P′) have a strong influence on C_{PK}, but the equation is slightly more sensitive to L/W than H/(P+P′). The same was also discovered for the power coefficients of L/W and H/(P+P′) in Eq. (7).

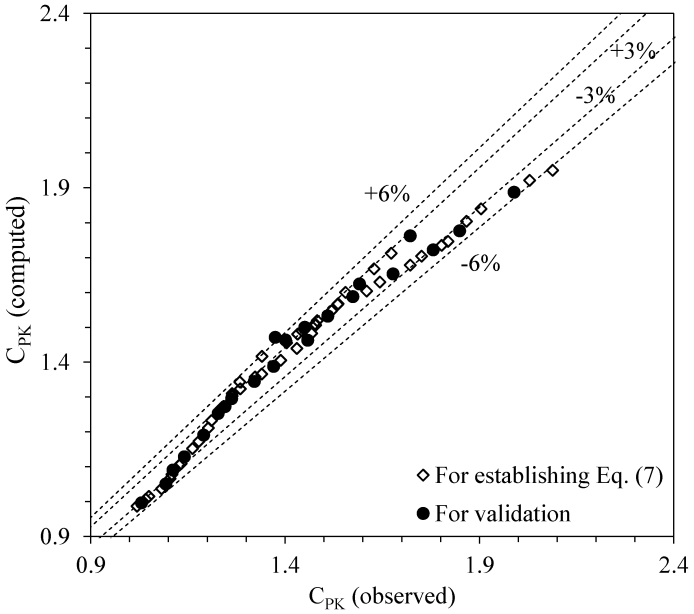

Fig. 4 Checking the accuracy of the proposed equation under the free-flow condition, Eq. (7)

Table 3
Sensitivity analysis: R^2 for different combinations of independent variables

Independent variable		R^2
L/W	H/(P+ P′)	
Y	Y	0.973
Y	N	**0.694**
N	Y	0.604

* Y = Yes, N = No.

4.2 Proposed equations for the coefficient of discharge under the submerged flow condition

The following equation for the coefficient of discharge under the submerged flow condition was developed using the least squares technique and 69 datasets collected in the present study:

$$\frac{C_{PKs}}{C_{PK}} = 1.168 - 0.016\left(\frac{L}{W}\right) - 0.92\left(\frac{H_d}{H}\right) + 2.05\left(\frac{H_d}{H}\right)^2 - 1.825\left(\frac{H_d}{H}\right)^3 \le 1.0 \qquad (R^2 = 0.98) \qquad (8)$$

The R^2 of the above equation is 0.98. A total of 35 datasets were used to validate Eq. (8). Figure 5a shows a comparison of the computed C_{PK} using Eq. (8) with the observed values both for training and for validation. It was found that approximately 76.8% and 62.9% of the training and validation data, respectively, lie in the ± 5% error bands, while 100% of the data lie in the ± 10% error bands for both sets. For the 35 validation datasets, the maximum error is 9.03%, and the MAPE is 4.27%, while the RMSE = 0.033, which indicates the good performance of Eq. (8). Equation (8) is a little more complex than Eq. (9) but is applicable for H_d/H up to approximately 1.0.

The following simplified formula, comparable to that suggested by Villemonte [29] for rectangular shaped weirs, was established using the 44 datasets collected in this study

$$\frac{C_{PKs}}{C_{PK}} = \left(1 - \left(\frac{H_d}{H}\right)^{2.28}\right)^{0.3} \le 1.0 \qquad (R^2 = 0.93) \qquad (9)$$

The R^2 of Eq. (9) is 0.93. A grid search method was applied to the dissimilar values of the hyperparameters. The R^2 and MAPE for these dissimilar hyperparameters were obtained to find the best solution. Therefore, a large set of R^2 values was obtained depending on different values of the hyperparameters, and the optimal set was chosen. The best value of R^2 in this state is 0.93 for $a_1 = 2.28$, $b_1 = 0.3$ and $c_1 = 1.0$. Likewise, if $a_1 = 1.0$, $b_1 = 0.21$ and $c_1 = 1.07$, R^2 equals 0.91, which is not as good as $R^2 = 0.93$. A total of 22 datasets were used to validate each of the equations obtained for different combinations of hyperparameters. Figure 5b shows a comparison of the computed C_{PK} using Eq. (9) with the observed values both for training and for validation. It was found for Eq. (9) that approximately 84.1% and 81.8% of the training and validation data, respectively, lie in the ± 5% error bands, while 97.7% and 95.4% of the data lie in the ± 10% error bands. However, this equation is strictly applicable only for H_d/H up to 0.9. For the 22 validation datasets, the maximum error and MAPE are 11.32% and 2.94%, respectively, while RMSE = 0.0289. While analysing the data used for Eqs. (8) – (9), it was observed that most of the results lie within ± 5% for both equations, as shown in Figs. 5a and 5b and discussed above. However, the maximum error is slightly higher for Eq. (9). The errors are within a considerable range, and the equations perform well.

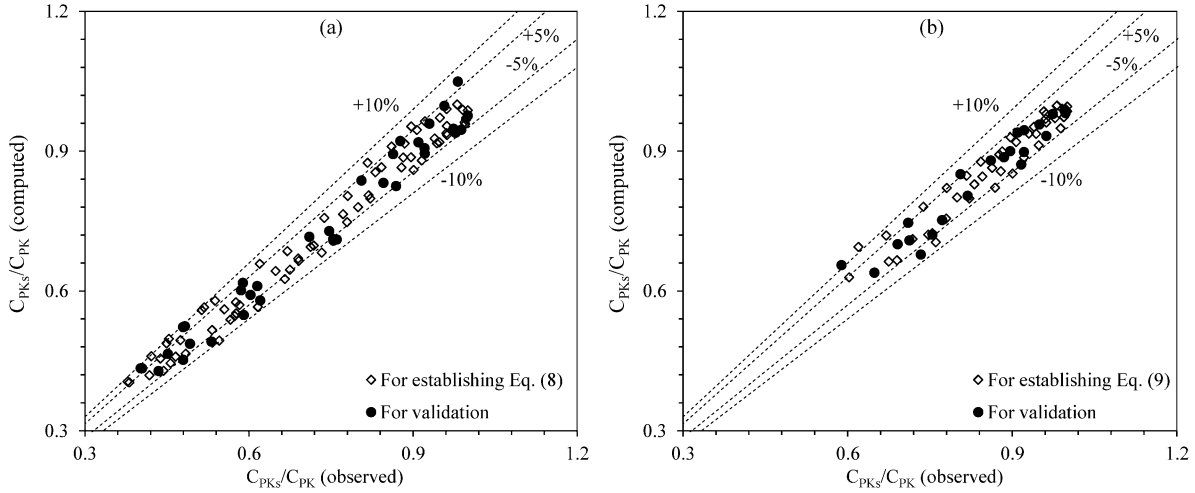

Fig. 5 a Checking the accuracy of the proposed Eq. (8), and **b** Checking the accuracy of the proposed Eq. (9)

4.3 Siltation effect

The construction of a hydraulic structure across a river leads to a change in the flow configuration and induces siltation upstream of the structure. It is apparent that such siltation affects the discharge capacity of a PK weir; however, this aspect has not been investigated to date. In the present investigation, tests were carried out with siltation upstream of the weir extending up to the sill of the inlet key for three different PK models having distinct dimensions. For each of the three PK weir models (PKN_1, PKN_2, and PKN_3), the first set of experiments was conducted considering no siltation on the upstream side, whereas the second set was performed considering siltation reaching a height $P' = 0.035$ m. For each experimental run, Q and H were measured, and C_{PK} was calculated using Eq. (1). Photometric views of the free-flowing (left) and submerged (right) PK weirs with upstream siltation are depicted in Fig. 6.

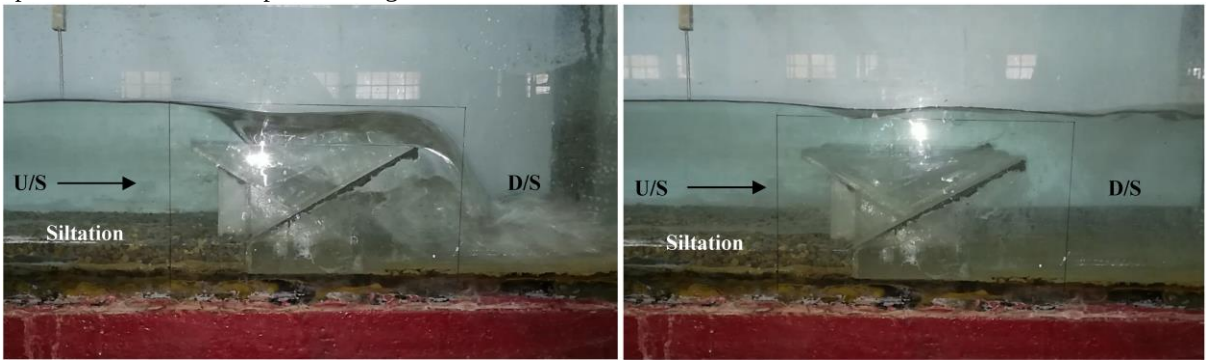

Fig. 6 Photometric views of free-flow (left) and submerged flow (right) conditions under upstream siltation

4.3.1 Free-flow condition

Figures 7a, 7b and 7c show the variations in C_{PK} versus H/P for the cases both with and without siltation upstream of the three PK weir models under the free-flow condition. For low H/P values (≤ 0.34), there is a limited effect of upstream siltation on the coefficient of discharge. However, considerable deviation is observed

for H/P values ≥ 0.34. A maximum decrease of an approximately 4% in C_{PK} is found due to sedimentation on the upstream side in the case of PKN_1. Figures 7b and 7c depict less deviation between the C_{PK} versus H/P graphs obtained for the siltation and no siltation cases for the free-flowing PKN_2 and PKN_3 models than that observed for the PKN1 model. A change of nearly 3% is noticed for PKN_2 and PKN_3 weirs. The deviation decreases at higher values of H/P, as seen in Figs. 7a, 7b and 7c, when the tailwater submergence starts to affect the flow condition. These deviations may be minor but should not be neglected in the case of channels that carry a high sediment load and may result in upstream siltation after placing a PK weir.

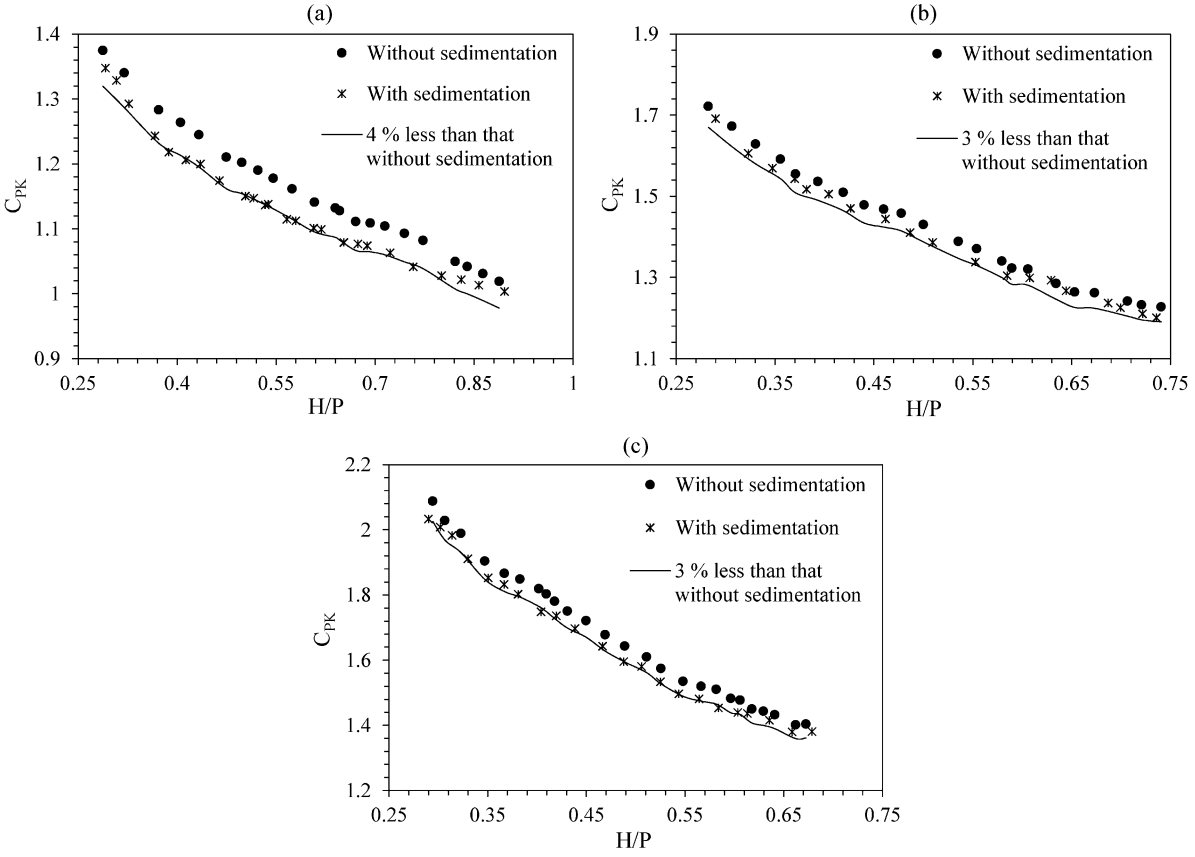

Fig. 7 a Variation in C_{PK} versus H/P for PKN_1, **b** Variation in C_{PK} versus H/P for PKN_2, and **c** Variation in C_{PK} versus H/P for PKN_3

The following equation for the coefficient of discharge under the free-flow condition with upstream siltation was developed using the least square technique and 44 datasets collected in the present study:

$$C_{PK'} = 0.645\left(\frac{L}{W}\right)^{0.415}\left(\frac{H}{P}\right)^{-0.352} \qquad (R^2 = 0.98) \qquad (10)$$

where $C_{PK'}$ is the coefficient of discharge for the case with upstream siltation up to the sill of the inlet key. The R^2 for the above equation is 0.98. A total of 23 datasets were used to validate Eq. (10). Figure 8 shows a comparison between the computed $C_{PK'}$ using Eq. (10) and the observed values both for training and for validation. It was found that approximately 70.5% and 56.5% of the training and validation data, respectively, lie in the ± 3% error bands, while 97.7% and 100% of the data lie in the ± 6% error bands. The ranges of the different variables are listed in Table 2, and a/b is approximately 1.2. The maximum error and MAPE for the datasets used in validation are 5.6% and 2.45%, respectively, and the RMSE is 0.043.

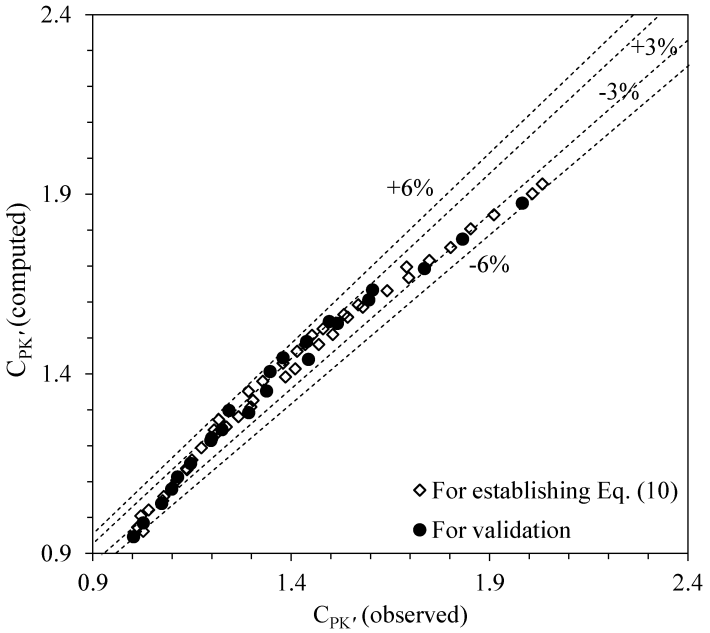

Fig. 8 Checking the accuracy of the equation proposed for free-flow condition with upstream siltation, Eq. (10).

4.3.2 Submerged flow condition

For PK weirs, the modular submergence range was found at $H_d/H < 0.6$ by Kabiri-Samani and Javaheri [10], $H_d/H < 0.48$ by Dabling and Tullis [26] and $H_d/H < 0.5$ (for Type-A) by Cicero and Delisle [15]. In the present study, the experimental data collected for all three PK weir models with upstream siltation were used to plot the variations in $C_{PKs}/C_{PK'}$ with H_d/H, as shown in Fig. 9. For PKN_1 with L/W = 2.3, two discharges of 8.3×10^{-3} m^3/s and 17.6×10^{-3} m^3/s were taken into account, whereas for PKN_2 with L/W = 3.6, Q = 10.33×10^{-3} m^3/s and 17.75×10^{-3} m^3/s were considered, and for PKN_3 with L/W= 4.9, plots were drawn for discharges of 13.06×10^{-3} m^3/s and 18.5×10^{-3} m^3/s. The submergence generally affected the coefficient of discharge for $H_d/H \geq 0.5$. Therefore, the modular submergence range is $H_d/H < 0.5$, which is close to the range of previous studies.

Figure 10 shows a negligible effect of siltation on the discharge capacity of PK weirs under the submerged flow condition, which indicates that during events with very high flood levels, the effect of upstream siltation will be very minor. Models with different L/W values and different cases, i.e., with siltation (with silt) and without siltation (w/o silt), were considered in this study. In each case, data were collected for two discharges to obtain better results. For L/W = 2.3 and Q = 8.3×10^{-3} m^3/s (with silt and w/o silt on the upstream side of the weir), there is almost no deviation between the plots: the two plots coincide with each other. Similarly, when the discharge value was 17.6×10^{-3} m^3/s and L/W = 2.3, no sign of change appeared in the graphs for either case. On the other hand, for the PK weir with L/W = 3.6, an insignificant deviation between the plots is observed at Q = 10.07×10^{-3} m^3/s and 10.33×10^{-3} m^3/s. A similar scenario is witnessed for the discharge values of 17.94×10^{-3} m^3/s and 17.75×10^{-3} m^3/s. Finally, the plots for the three-cycle PK weir (L/W = 4.9, Q = 13.5×10^{-3} m^3/s and 13.06×10^{-3} m^3/s) show very little deviation. It was already observed that there is a negligible effect of upstream siltation on the discharge capacity of the PK weir under the submerged flow condition, so Eq. (8) may be used for cases both with and without upstream siltation.

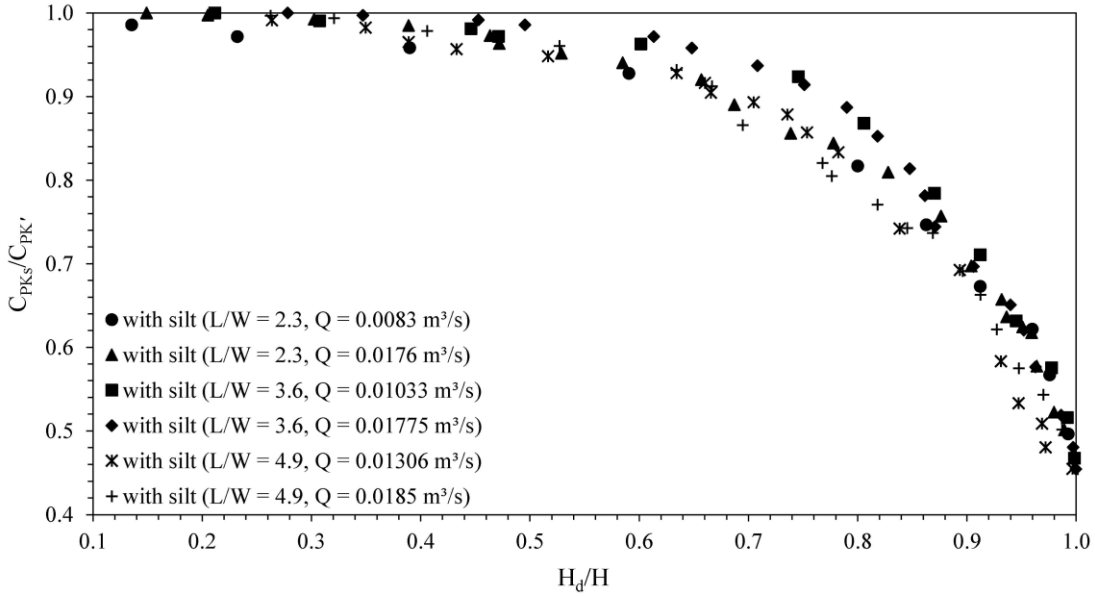

Fig. 9 Variations in $C_{PKs}/C_{PK'}$ versus H_d/H for different L/W and discharge values considering upstream siltation

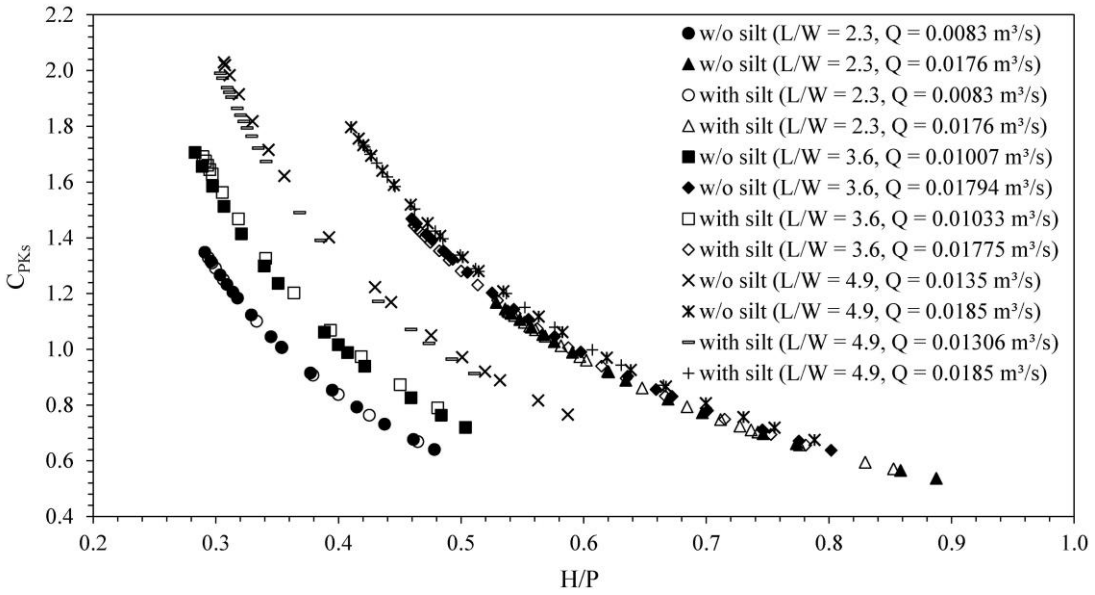

Fig. 10 Variations in C_{PKs} for different L/W and discharge values (with and without siltation)

5 Conclusions

Experiments were performed to study the discharge capacities of PK weirs (with noses below the outlet apexes) with and without upstream siltation under free-flow and submerged flow conditions, and empirical equations were established to estimate the coefficients of discharge of PK weirs for such cases. Precise discharge and head measuring instruments were used to limit experimental uncertainties. It was observed that upstream siltation has a considerable effect on the discharge capacity of a free-flowing PK weir for $H/P \geq 0.34$. However, the siltation effect starts to decrease at higher H/P values when tailwater submergence starts to affect the PK weir flow condition. Siltation does not affect the discharge capacity of a submerged PK weir. Maximum decreases in the coefficient of discharge of 4% for the 1-cycle model and 3% for the other two models were found. These deviations may be low but are not negligible. Such a study has not been conducted previously, and the findings will contribute considerably to future developments in PK weirs. Planners and designers must not avoid such reductions in channels that carry a high sediment load, which may result in upstream siltation after the placement of a PK weir. The proposed equations for free-flowing PK weirs perform very well with a maximum error of approximately 7% and an MAPE of approximately 2.5%. Approximately 60% of the data lie within the ± 3% error bands, and almost all data lie within the ± 6% error bands. These equations will be used efficiently within the parameter ranges listed in Table 2 and for a/b values of approximately 1.2. The submergence effect starts at an H_d/H of approximately 0.5, which is very close to the outcomes of previous studies. The equations proposed for submerged PK weirs also perform well with maximum errors of 9.0% for Eq. (8) and 11.32% for

Eq. (9). However, the MAPE (2.94%) and RMSE (0.0289) of Eq. (9) are better than those (4.27% and 0.033, respectively) of Eq. (8). These two equations are also useful for upstream siltation. Experiments were carried out considering an upstream bed (0.035 m high) composed of a gravel mixture with a median particle size of 0.0055 m; in the future, further research may be carried out with different particle sizes and upstream scouring conditions.

List of symbols

a	Inlet key width (m)
b	Outlet key width (m)
B	Sidewall overflowing crest length (m)
B_b	Base length of the PK weir (m)
B_i	Overhang length for the inlet key (m)
B_o	Overhang length for the outlet key (m)
C_{PK}	Coefficient of discharge for a PK weir with no siltation on the upstream side (–)
C_{PKs}	Coefficient of discharge of a submerged PK weir (–)
$C_{PK'}$	Coefficient of discharge for a PK weir with upstream siltation (–)
h	Flow depth over the crest (m)
h_v	Velocity head (m)
H	Total upstream head over the crest (m)
H_d	Total downstream hydraulic head (m)
L	Total crest length of the weir (m)
P	Height of inlet (P_i) and outlet keys (P_o) (m)
P´	Incoming flow depth below the inlet key sill (m)
Q	Discharge capacity of a PK weir (m^3/s)
Q_s	Discharge passing under the submerged condition (m^3/s)
T_s	Wall thickness (m)
W	Width of the weir (m)
y	Total upstream flow depth (m)
S_w	Submergence of a PK weir (–)
σ	Surface tension (N/m)
μ	Viscosity (Pa s)

Conflicts of interest

The authors hereby declare that they do not have any conflicts of interest

References

[1] Leite Ribeiro M., Pfister M., Schleiss A. J., and Boillat J. L., "Hydraulic design of a-type piano key weirs", Journal of Hydraulic Research, 2012; 50 (4), 400-408.

[2] Lempérière F., and Ouamane A, "The Piano Keys weir: A new cost-effective solution for spillways", International Journal on Hydropower and Dams, 2003; 10 (5), 144-149.

[3] Leite Ribeiro M., Bieri M., Boillat J. L., Schleiss A. J., Singhal G., and Sharma N., "Discharge Capacity of Piano Key Weirs", Journal of Hydraulic Engineering, 2012; 138 (2), 199-203.

[4] Singhal G. D., and Sharma, N. Rehabilitation of Sawara Kuddu Hydroelectric Project – Model studies of Piano KeyWeir in India, Proceedings of the International Conference on Labyrinth and Piano Key Weirs – PKW 2011, Liege, Belgium, CRC Press, London, 2011, 241-250.

[5] Noseda M., Stojnic I., Pfister M., and Schleiss A. J., "Upstream Erosion and Sediment Passage at Piano Key Weirs", Journal of Hydraulic Engineering, 2019; 145 (8), 04019029.

[6] Laugier F., "Design and construction of the first Piano Key Weir spillway at Goulours dam", International Journal on Hydropower and Dams, 2007; 14 (5), 94-101.

[7] Erpicum S., Archambeau P., Dewals B., and Pirotton M. Hydraulics of Piano Key Weirs: A review, Proceedings of the 3rd International Workshop on Labyrinth and Piano Key Weirs (PKW 2017), Qui Nhon, Vietnam, CRC Press, London, 2017, 27-36.

[8] Crookston B. M., Erpicum S., Tullis B. P., and Laugier F., "Hydraulics of Labyrinth and Piano Key Weirs: 100 Years of Prototype Structures, Advancements, and Future Research Needs", Journal of Hydraulic Engineering, 2019; 145 (12), 02519004.

[9] Lempérière F., Vigny J. P., and Ouamane A. General comments on Labyrinths and Piano KeyWeirs: The past and present, Proceedings of the International Conference on Labyrinth and Piano Key Weirs – PKW 2011, Liege, Belgium, CRC Press, London, 2011, 17-24.

[10] Kabiri-Samani A., and Javaheri A., "Discharge coefficients for free and submerged flow over Piano Key weirs", Journal of Hydraulic Research, 2012; 50 (1), 114-120.

[11] Oertel M. Piano Key Weir Research : State-of-the-art and Future Challenges, 7th IAHR International Symposium on Hydraulic Structures, Aachen, Germany, Utah State University, 2018, 474-481.
[12] Anderson R. M., and Tullis B. P., "Piano Key Weir Hydraulics and Labyrinth Weir Comparison", Journal of Irrigation and Drainage Engineering, 2013; 139 (3), 246-253.
[13] Anderson R. M., and Tullis B. P., "Comparison of Piano Key and Rectangular Labyrinth Weir Hydraulics", Journal of Hydraulic Engineering, 2012; 138 (4), 358-361.
[14] Belaabed F., and Ouamane A. Submerged flow regimes of Piano Key weir, Proceedings of the Second International Workshop on Labyrinth and Piano Key Weirs -PKW 2013, Paris, France, CRC Press, London, 2013, 85-92.
[15] Cicero G. M., and Delisle J. R. Discharge characteristics of piano key weirs under submerged flow, Proceedings of the Second International Workshop on Labyrinth and Piano Key Weirs -PKW 2013, Paris, France, CRC Press, London, 2013, 101-109.
[16] Crookston B. M., Anderson R. M., and Tullis B. P., "Free-flow discharge estimation method for Piano Key weir geometries", Journal of Hydro-environment Research, 2018; 19, 160-167.
[17] Karimi Chahartaghi M., Nazari S., and Shooshtari M. M., "Investigating the effect of a parapet wall on the hydraulic performance of an arced piano key weir", Journal of Hydraulic Research, 2019; 58 (2), 274-282.
[18] Kumar B., Kadia S., and Ahmad Z., "Evaluation of discharge equations of the piano key weirs", Flow Measurement and Instrumentation, 2019; 68, 101577.
[19] Laugier F., Pralong J., and Blancher B. Influence of structural thickness of sidewalls on PKW spillway discharge capacity, Proceedings of the International Conference on Labyrinth and Piano Key Weirs – PKW 2011, Liege, Belgium, CRC Press, London, 2011, 159-165.
[20] Lempérière F. New labyrinth weirs triple spillways discharge, Dams, Piano Keys Weirs, Tidal Energy & Energy Storage - http://www.hydrocoop.org, 2009.
[21] Li G., Li S., and Hu Y., "The effect of the inlet/outlet width ratio on the discharge of piano key weirs", Journal of Hydraulic Research, 2019; 58 (4), 594-604.
[22] Machiels O., Erpicum S., Archambeau P., Dewals B., and Pirotton M. Piano Key weir preliminary design method: Application to a new dam project, Proceedings of the International Conference on Labyrinth and Piano Key Weirs – PKW 2011, Liege, Belgium, CRC Press, London, 2011, 199-206.
[23] Machiels O., Erpicum S., Archambeau P., Dewals B., and Pirotton M., "Parapet Wall Effect on Piano Key Weir Efficiency", Journal of Irrigation and Drainage Engineering, 2013; 139 (6), 506-511.
[24] Machiels O., Pirotton M., Pierre A., Dewals B., and Erpicum S., "Experimental parametric study and design of Piano Key Weirs Experimental parametric study and design of Piano Key Weirs", Journal of Hydraulic Research, 2014; 52 (3), 326-335.
[25] Pfister M., and Schleiss A. J. Effect of driftwood on hydraulic head of Piano Key weirs, Proceedings of the Second International Workshop on Labyrinth and Piano Key Weirs -PKW 2013, Paris, France, CRC Press, London, 2013, 255-264.
[26] Dabling M. R., and Tullis B. P., "Piano key weir submergence in channel applications", Journal of Hydraulic Engineering, 2012; 138(7), 661-666.
[27] Tullis B. P., Young J. C., and Chandler M. A., "Head-Discharge Relationships for Submerged Labyrinth Weirs", Journal of Hydraulic Engineering, 2007; 133 (3), 248-254.
[28] Kabiri-Samani A., Ansari A., and Borghei S. M., "Hydraulic behaviour of flow over an oblique weir", Journal of Hydraulic Research, 2010; 48 (5), 669-673.
[29] Villemonte J. R., "Submerged weir discharge studies", Engineering news record, 1947; 139 (26), 54–57.
[30] Erpicum S., Tullis B. P., Lodomez M., Archambeau P., Dewals B. J., and Pirotton M., "Scale effects in physical piano key weirs models", Journal of Hydraulic Research, 2016; 54 (6), 692-698.
[31] Tullis B. P., Crookston B. M., and Young N., "Scale Effects in Free-Flow Nonlinear Weir Head-Discharge Relationships", Journal of Hydraulic Engineering, 2020; 146 (2), 04019056.
[32] Novak P., and Cabelka J. Models in hydraulic engineering: physical principles and design applications, Pitman Publishing Ltd, Boston, 1981.
[33] Henderson F. M. Open channel flow. Macmillan, New York, 1966.
[34] Jüstrich S., Pfister M., and Schleiss A. J., "Mobile Riverbed Scour Downstream of a Piano Key Weir", Journal of Hydraulic Engineering, 2016; 142 (11), 04016043.